CHAPTER 4

RESULTS AND DISCUSSION

This chapter presents the results of the experiments described in the preceding chapter and demonstrates that nitrogen dissolution in the molten weld pool during autogenous arc welding is influenced to a significant extent by the nitrogen content of the shielding gas and the chemical composition of the weld metal, in particular the base metal nitrogen content prior to welding and the surface active element concentration.

4.1 THE WELD POOL TEMPERATURE DURING WELDING

A typical experimentally measured temperature profile, represented by the recorded thermoelectric voltage signal from a thermocouple immersed in the molten weld pool, is shown in Figure 4.1. The temperature measured by the thermocouple increases rapidly on insertion in the weld pool, and then stabilises at a plateau value that was assumed to be equal to the temperature of the central region of the weld pool. On removal of the thermocouple from the molten metal, the measured temperature rapidly decreases to ambient temperature, as shown in Figure 4.1.

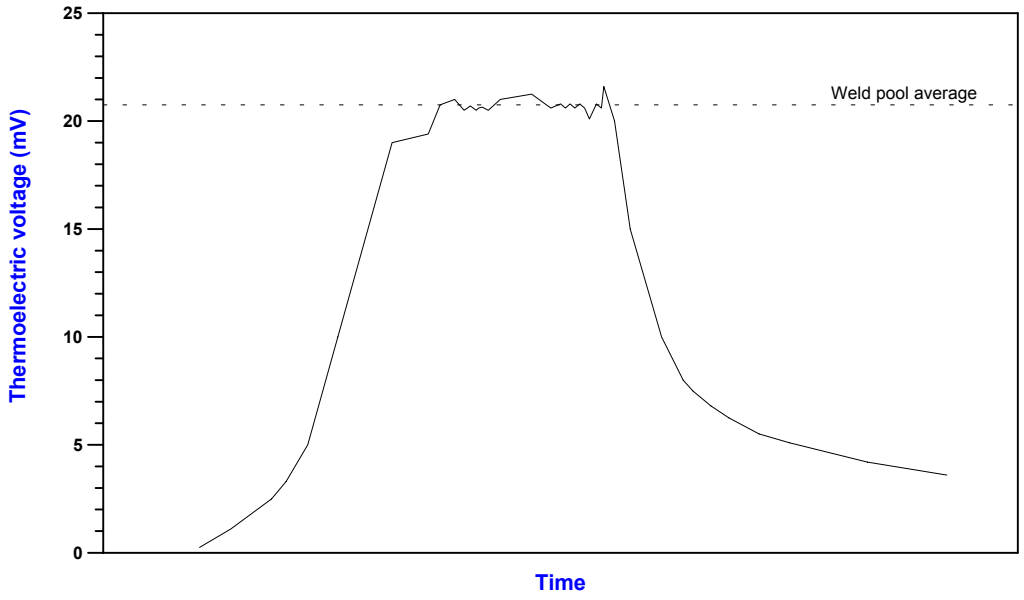

Figure 4.1 Typical thermoelectric voltage signal measured by a thermocouple inserted in the weld pool.

As described in §3.3, four weld pool temperature measurements were performed – two at a welding current of 300 A and two more at a welding current of 350 A. The four measurements yielded an average weld pool temperature of 1722°C ± 14°C. The results were very repeatable and no significant differences were detected between the temperatures measured at the two different welding currents. The difference

between the measured temperature and the liquidus temperature (the liquidus temperature of the experimental type 310 alloys is approximately 1500°C[1]) is greater than the 100°C difference proposed by Kuwana *et al*[2] in equation (1.23), but this can probably be attributed to a difference in the welding parameters (arc voltage and travel speed) employed by these authors, as compared to the current investigation. The experimentally measured weld pool temperature can now be substituted into equations (1.4) and (1.5) in the literature survey to calculate the equilibrium nitrogen solubility limit at the relevant nitrogen partial pressures in each of the experimental alloys.

4.2 THE INFLUENCE OF THE SHIELDING GAS NITROGEN CONTENT ON THE NITROGEN SOLUBILITY OF STAINLESS STEEL WELDS

4.2.1 Visual observations

Except for Cromanite and VFA 755 (the high nitrogen, high sulphur experimental alloy), no evidence of porosity or degassing was found in any of the samples welded in pure argon or argon-1,09% N_2 mixtures. The welds generally exhibited smooth profiles with very little ripple formation on the surface. An example of such a weld is shown in Figure 4.2. The Cromanite welds, however, showed severe porosity after welding in pure argon and Ar-1,09% N_2 shielding gas mixtures, often containing blow holes with diameters in excess of 1 mm (as shown in Figure 4.3). Autogenous welding of Cromanite in the presence of these shielding gases was also associated with unstable weld pools, severe spattering, flashes of light, a hissing sound and the violent expulsion of liquid metal droplets from the weld pool. Extreme cases of such instability resulted in the formation of a deposit on the surface of the tungsten electrode. Bennett and Mills[3] studied the weldability of a number of nitrogen-containing austenitic stainless steels and found this electrode deposit to be rich in tungsten, containing iron, chromium, manganese and some silicon. They attributed this behaviour to the evolution of nitrogen from the liquid metal that expels molten droplets from the weld pool during welding. The conclusion can be drawn that the nitrogen solubility limit in Cromanite was exceeded during welding, resulting in the nucleation of nitrogen bubbles in the weld pool. Some of these bubbles escaped, causing spatter and metal expulsion, while some were trapped by the advancing solidification front, resulting in the formation of blow holes in the solidified weld metal. The Cromanite weld metal appeared to be very viscous during welding, exhibiting coarse ripples and irregular bead surfaces after solidification. VFA 755 displayed smooth weld pool profiles and porosity-free welds after welding in pure argon, but spattering and bubble formation became evident with the addition of 1,09% nitrogen to the shielding gas.

At higher nitrogen levels in the shielding gas (i.e. 5,3% N_2, 9,8% N_2 and 24,5% N_2) all the alloys evaluated, including Cromanite and type 304 stainless steel, exhibited unstable weld pools and spattering during welding, resulting in uneven weld surfaces and visible porosity after welding. An increase in the base metal nitrogen concentration of the experimental alloys appeared to increase the amount of degassing and spattering during welding, whereas an increase in the shielding gas nitrogen content raised the amount of porosity in the welds. An example of such a weld is shown in Figure 4.4. The Cromanite

welds, however, exhibited less visible porosity, although welding was associated with violent gas evolution, spattering, flashes and very uneven weld profiles (as shown in Figure 4.5). This indicates that nitrogen was evolved from the weld pool during welding, even though less porosity was visible in the weld metal after welding. Although the presence of blowholes in the weld metal confirms that nitrogen desorption occurred during welding, it must be emphasised that the absence of porosity after solidification does not rule out the possibility that nitrogen evolution took place. Degassing and bubble formation were often observed during the welding of samples that displayed no visible porosity after cooling. It is postulated that any nitrogen bubbles formed in these welds escaped to the atmosphere prior to solidification, causing the observed spattering and flashing phenomena. As a result, the presence or absence of porosity in the weld metal after welding cannot be used to gauge whether nitrogen desorption took place during welding. Visual observation of the molten weld pool proved to be a more accurate way of determining whether nitrogen bubble evolution occurred.

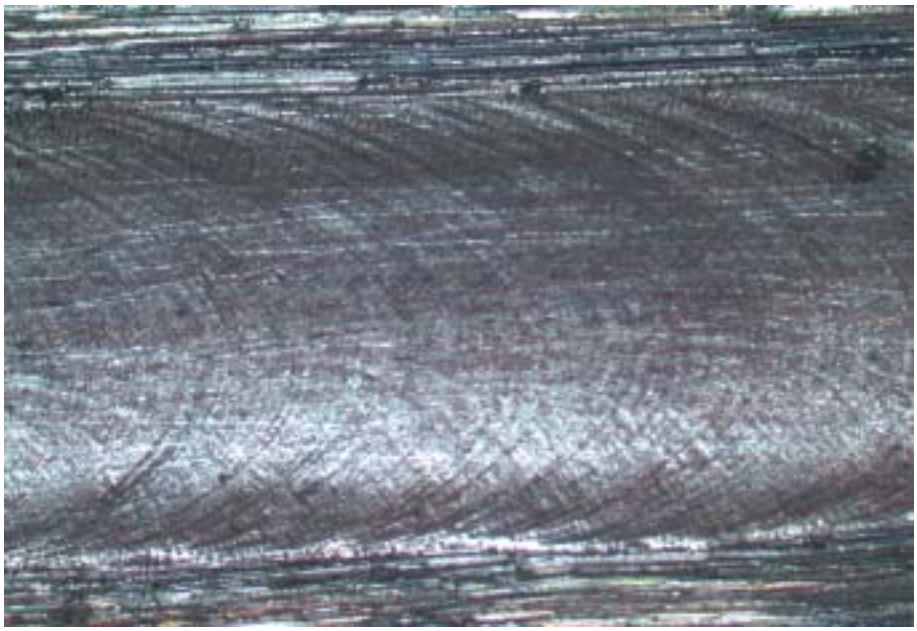

Figure 4.2 Surface appearance of VFA 752 (low N, high S) welded in pure argon. Magnification: 8x.

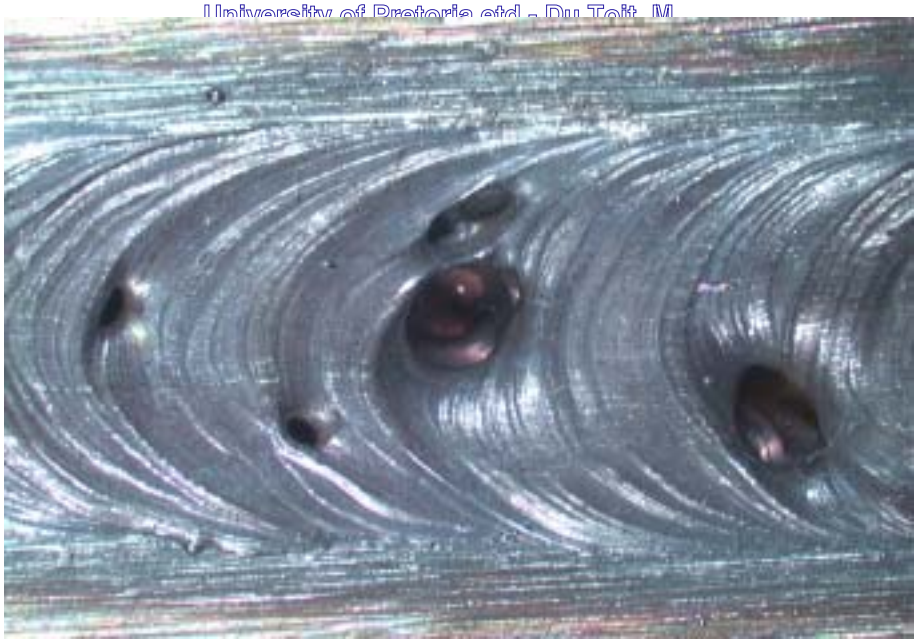

Figure 4.3 Surface appearance of Cromanite welded in pure argon. Magnification: 8x.

Figure 4.4 Surface appearance of VFA 752 (low N, high S) welded in an Ar-24,5%N_2 shielding gas atmosphere. Magnification: 8x.

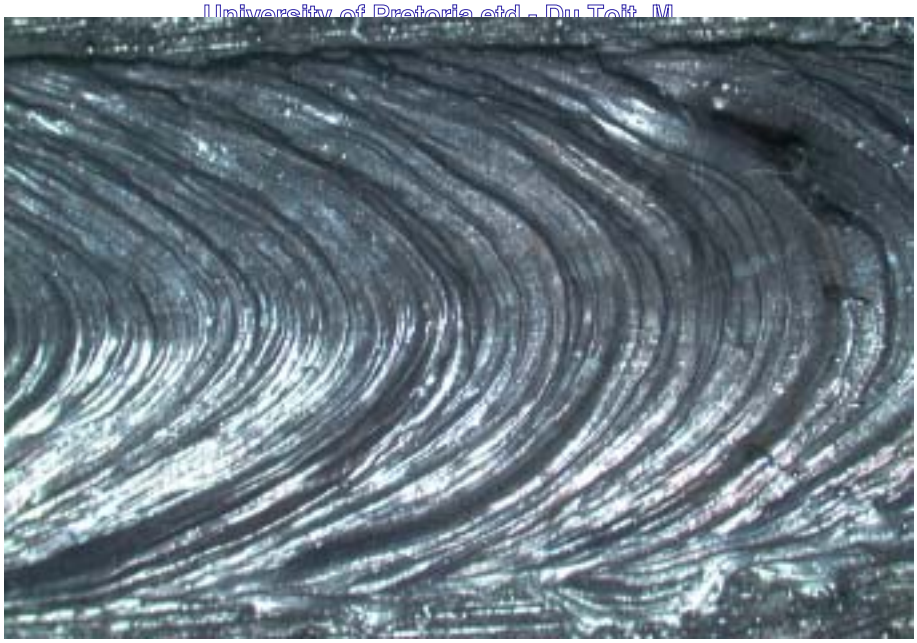

Figure 4.5 Surface appearance of Cromanite welded in an Ar-24,5%N_2 shielding gas atmosphere. Magnification: 8x.

4.2.2 Weld metal nitrogen contents

The average weld metal nitrogen contents measured in the different samples are given in Table 4.1, and represented graphically in Figures 4.6, 4.7 and 4.8 for the low sulphur, high sulphur and commercial alloys (Cromanite and AISI 304), respectively. The equilibrium nitrogen solubility limit, also shown in Figures 4.6, 4.7 and 4.8, was calculated at the measured weld pool temperature (1722°C) for each nitrogen partial pressure using Wada and Pehlke's coefficients and interaction parameters[4].

Table 4.1 Average weld metal nitrogen contents of the different welded samples (percentage by mass).

Alloy	Comments	Base metal N content	Weld metal N content for various shielding gas compositions				
			Pure Ar	Ar-1,09%N_2	Ar-5,3%N_2	Ar-9,8%N_2	Ar-24,5%N_2
VFA 657	Low N, low S	0,005%	0,017%	0,082%	0,196%	0,242%	0,257%
VFA 658	Medium N, low S	0,105%	0,105%	0,166%	0,230%	0,245%	0,270%
VFA 659	High N, low S	0,240%	0,216%	0,240%	0,267%	0,265%	0,277%
VFA 752	Low N, high S	0,006%	0,016%	0,082%	0,180%	0,184%	0,194%
VFA 753	Medium N, high S	0,097%	0,118%	0,150%	0,220%	0,230%	0,226%
VFA 755	High N, high S	0,280%	0,271%	0,280%	0,331%	0,325%	0,330%
Cromanite	-	0,511%	0,433%	0,450%	0,528%	0,550%	0,686%
AISI 304	-	0,078%	0,094%	0,172%	0,240%	0,303%	0,336%

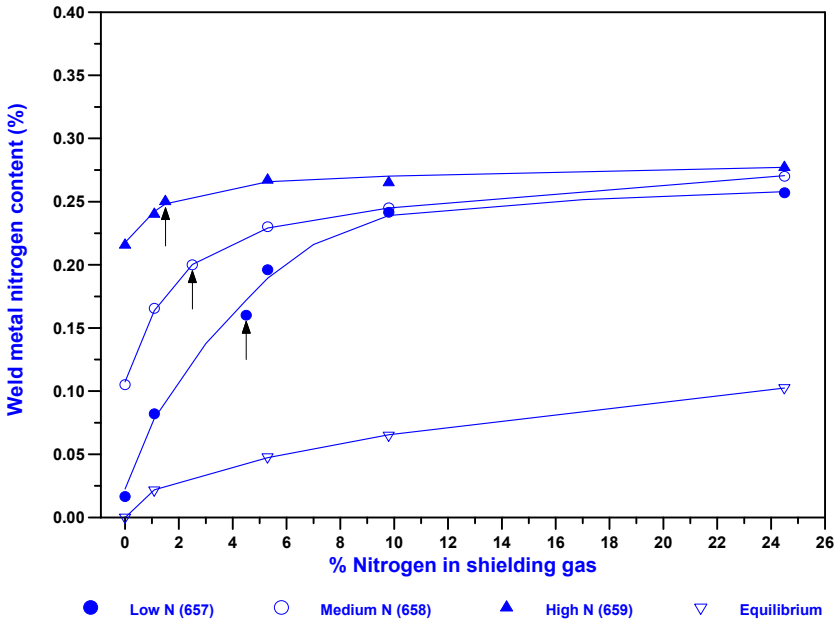

Figure 4.6 Weld metal nitrogen concentration as a function of the shielding gas nitrogen content for the experimental low sulphur alloys. The arrows indicate the onset of bubble formation during welding.

The influence of nitrogen additions to argon shielding gas on the nitrogen content of the autogenous welds appears to be consistent with that described in literature for carbon steels and stainless steels (refer to Figures 1.5, 1.6 and 1.20). The weld metal nitrogen content initially increases as the shielding gas nitrogen content increases, and then reaches a constant steady-state value that is independent of the actual nitrogen partial pressure. This steady-state level is associated with a dynamic equilibrium where the rate of absorption of nitrogen is balanced by the evolution of nitrogen from the melt[5]. At all nitrogen partial pressures investigated the nitrogen content of the weld metal exceeds the equilibrium solubility limit calculated at the weld pool temperature. This is consistent with available literature[5,6,7,8] and confirms that

Sievert's law is not obeyed during arc welding. The high nitrogen solubility limit in the presence of an arc plasma is generally attributed to the presence of monatomic nitrogen in the arc[8,9,10].

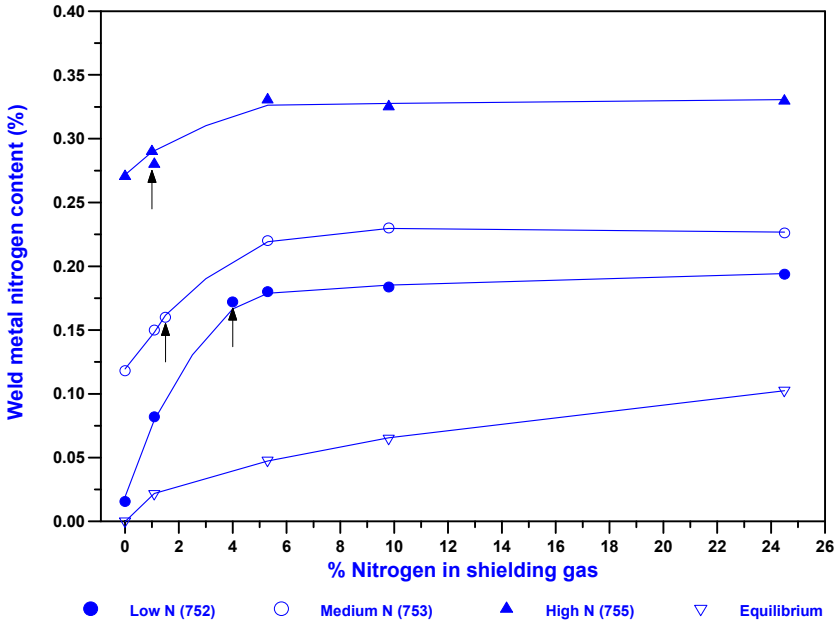

Figure 4.7 Weld metal nitrogen concentration as a function of the shielding gas nitrogen content for the experimental high sulphur alloys. The arrows indicate the onset of bubble formation during welding.

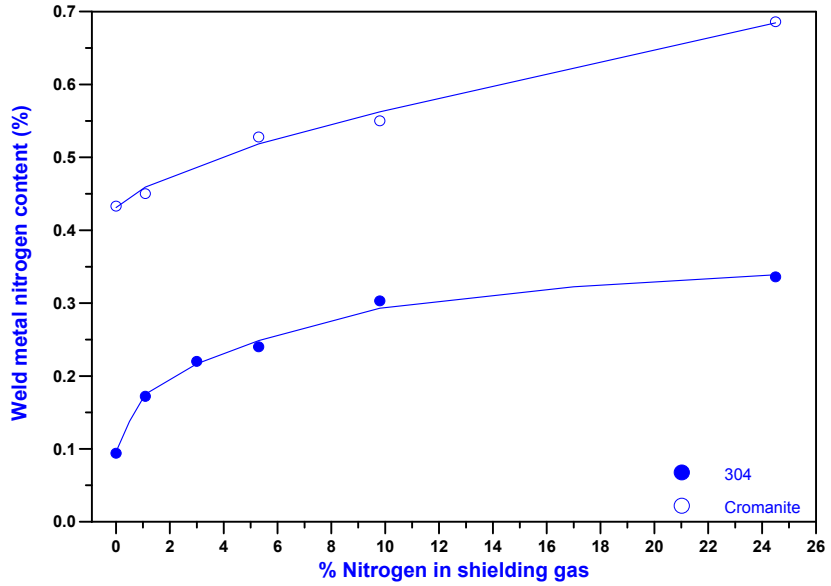

Figure 4.8 Weld metal nitrogen concentration as a function of the shielding gas nitrogen content for the commercial alloys.

It is interesting to note that the influence of the base metal nitrogen content on the absorption and desorption of nitrogen during welding appears to be dependent on the surface active element

concentration in the metal. In the case of the low sulphur alloys (Figure 4.6), an increase in the initial nitrogen level of the base metal causes an increase in the weld metal nitrogen content at low nitrogen partial pressures in the shielding gas. At higher nitrogen partial pressures, the nitrogen content of the welds approaches a steady-state value that is very similar for all three low sulphur alloys and virtually independent of the base metal nitrogen content. In the case of the high sulphur alloys (Figure 4.7), an increase in the base metal nitrogen content results in higher weld metal nitrogen contents over the entire range of nitrogen partial pressures evaluated, including a significant increase in the steady-state nitrogen concentration. This is contrary to the conclusions of Okagawa *et al*[11] and Suutala[12] who reported that the nitrogen content of welds is not influenced by the base metal nitrogen content prior to welding. This inconsistency can probably be attributed to the low base metal nitrogen and sulphur levels in the alloys studied by these authors (0,025% N and 0,009% S in the alloys studied by Okagawa *et al*[11] and between 0,008 and 0,076% N in the alloys investigated by Suutala[12]).

In order to explain the results described above, Figures 4.6 and 4.7 were redrawn in the form of Figures 4.9 and 4.10 to examine the influence of sulphur concentration on the low and high nitrogen alloys, respectively. Figure 4.9 shows that a high weld metal sulphur content reduces the steady-state nitrogen concentration in the case of the low nitrogen alloys (VFA 657 and VFA 752). This suggests that, in the absence of significant amounts of nitrogen in the base metal prior to welding, the surface active element concentration mainly influences the rate of nitrogen absorption from the arc atmosphere. The validity of this conclusion will be examined in Chapter 5. The sulphur content also has a significant influence on the weld metal nitrogen content in alloys containing high levels of base metal nitrogen (VFA 659 and VFA 755), with higher sulphur concentrations leading to considerably higher levels of nitrogen after welding (as shown in Figure 4.10). High base metal nitrogen contents also seem to increase the level of supersaturation in the weld metal over that required to nucleate nitrogen bubbles at atmospheric pressure. Since a higher sulphur concentration in the weld metal implies increased weld pool surface coverage, the higher nitrogen levels measured in the presence of an increased surface active element concentration suggest that, in the presence of high levels of base metal nitrogen, the nitrogen desorption reaction is retarded. This is consistent with the results shown in Figure 1.24 for iron-oxygen alloys, and with the findings of Battle and Pehlke[13] and Katz and King[10], who found the nitrogen desorption rate constant to be proportional to $(1-\theta_\Gamma)^2$, where $(1-\theta_\Gamma)$ is the total fraction of vacant surface sites (as shown in Figure 4.11). The influence of sulphur on the rate of nitrogen desorption during welding is expected to be more significant than its influence on the rate of the absorption reaction, since nitrogen evolution from the weld pool requires two surface sites for the adsorption and recombination of nitrogen atoms to form each N_2 molecule, whereas the absorption of monatomic nitrogen from the arc plasma requires only one surface site per atom dissolved (as shown in equations (1.10) to (1.12) in Chapter 1).

It is therefore postulated that a high nitrogen absorption rate in alloys with low base metal nitrogen contents, in conjunction with a high desorption rate in alloys with high base metal nitrogen levels, allows the weld metal nitrogen content of the low sulphur alloys to approach a steady-state value that is not influenced to any significant extent by the initial nitrogen content of the base metal (as shown in Figure

4.6). In the high sulphur alloys, the higher surface active element concentration retards the rate of nitrogen evolution from the weld pool by occupying a high fraction of the surface sites required for the recombination of nitrogen atoms to form N_2. As a result, more of the nitrogen initially present in the base metal is maintained in solution in the weld pool and the original nitrogen content is therefore expected to have a more significant influence on the subsequent weld nitrogen content (as confirmed by Figure 4.7). This is consistent with the results of Arata *et al*[14], who showed that the total weld metal nitrogen content is the sum of the residual nitrogen content of the base metal and any nitrogen picked up from the interaction between the shielding gas and the molten weld metal. The validity of these conclusions will be considered in Chapter 5 where the nitrogen absorption and desorption reaction rate constants are determined as a function of the surface active element concentration in the experimental alloys.

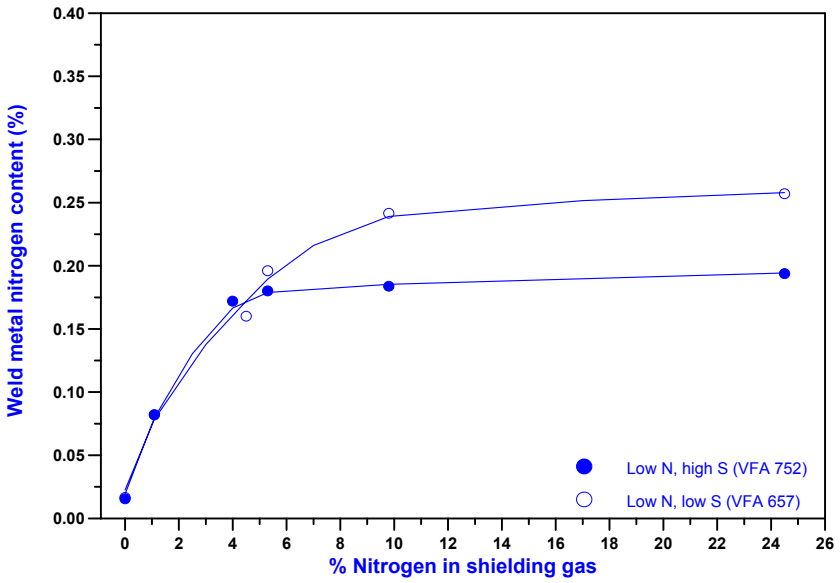

Figure 4.9 The influence of sulphur concentration on the weld metal nitrogen contents of the experimental low nitrogen alloys (VFA 657 and VFA 752).

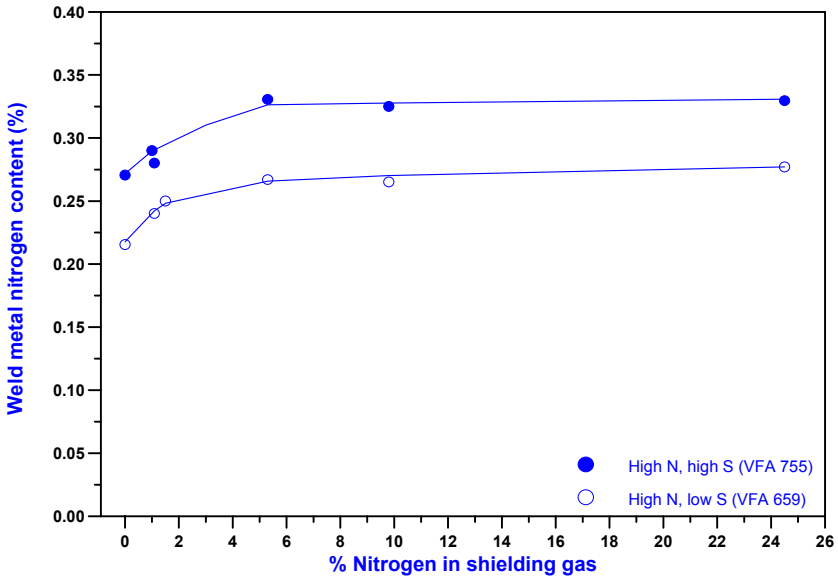

Figure 4.10 The influence of sulphur concentration on the weld metal nitrogen contents of the experimental high nitrogen alloys (VFA 659 and VFA 755).

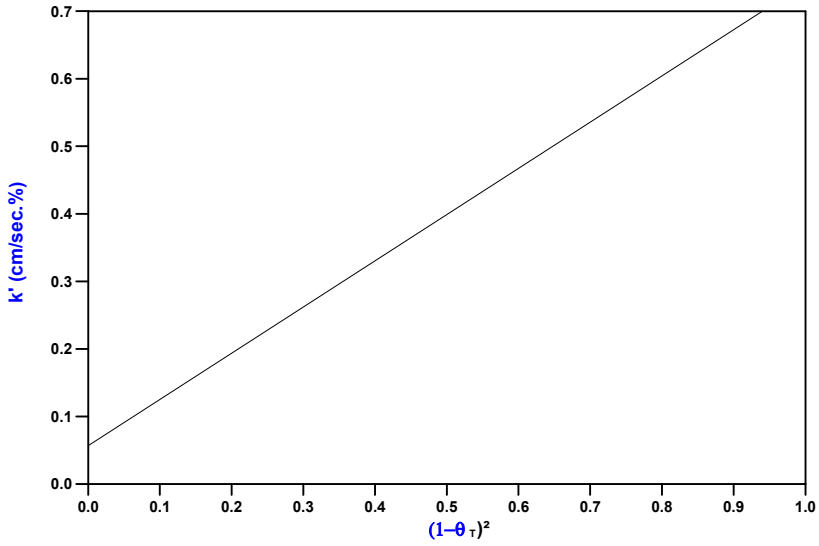

Figure 4.11 The initial apparent rate constant, k', for nitrogen desorption from liquid iron during plasma arc melting as a function of the surface availability, $(1-\theta_T)$[10].

The nitrogen contents of autogenous AISI 304 and Cromanite welds also increase with an increase in the nitrogen content of the shielding gas at low nitrogen partial pressures, followed by steady-state behaviour at higher partial pressures (Figure 4.8). The weld metal nitrogen content of Cromanite is significantly higher than that of AISI 304 over the entire range of partial pressures evaluated. This can be attributed to the higher initial nitrogen concentration in Cromanite, and the high chromium and manganese contents, which increase the nitrogen solubility limit in this steel. The rapid initial increase in the weld metal

nitrogen content with an increase in nitrogen partial pressure is not as evident in the case of Cromanite since steady-state behaviour initiates at a much lower shielding gas nitrogen content in this steel than in any of the other alloys investigated.

4.3 THE MINIMUM SHIELDING GAS NITROGEN CONTENT THAT LEADS TO NITROGEN BUBBLE FORMATION IN THE WELD POOL DURING WELDING

In order to determine the minimum shielding gas nitrogen content necessary to initiate steady-state behaviour, and consequently nitrogen bubble formation, in each of the alloys investigated, the shielding gas nitrogen content was increased from 0,5% to 5% in 0,5% increments during welding. The observed behaviour of the arc and weld pool during welding and the visual appearance of the completed weld as a function of the shielding gas nitrogen content are described in Table 4.2 (following page) for each of the alloys investigated (with the exception of Cromanite). Cromanite was not evaluated since it displays violent degassing and spattering, even in the absence of any nitrogen in the shielding gas during welding. Based on the visual observations described in Table 4.2, the minimum shielding gas nitrogen content that leads to nitrogen desorbtion and degassing from the weld pool and the corresponding weld metal nitrogen contents are shown in Table 4.3 for the experimental alloys and type 304.

Table 4.2 Experimental observations of the welding arc and weld pool during welding and the visual appearance of the completed weld of each of the experimental alloys and type 304 stainless steel as a function of the shielding gas nitrogen content during welding.

A. Alloy	Shielding gas composition									
	Ar - 0,5% N_2	Ar - 1,0% N_2	Ar - 1,5% N_2	Ar - 2,0% N_2	Ar - 2,5% N_2	Ar - 3,0% N_2	Ar - 3,5% N_2	Ar - 4,0% N_2	Ar - 4,5% N_2	Ar - 5,0% N_2
AISI 304	No degassing or visible porosity, smooth profile	No degassing or visible porosity, smooth profile	No degassing or visible porosity, smooth profile	Limited bubble formation, smooth profile, no porosity	Limited bubble formation and instability, smooth profile, no porosity	Spattering and degassing, no visible porosity	Periodic spattering and degassing, no visible porosity	Severe spattering and degassing, some visible porosity	Severe spattering and degassing, visible porosity	Severe spattering and degassing, visible porosity
VFA 657 Low N, low S	No degassing or visible porosity, smooth profile	No degassing or visible porosity, smooth profile	No degassing or visible porosity, smooth profile	No degassing or visible porosity, smooth profile	No degassing or visible porosity, smooth profile	No degassing or visible porosity, smooth profile	No degassing or visible porosity, smooth profile	Slight bubble formation and instability, no visible porosity, smooth profile	Degassing, pool instability and flashing, no spattering or visible porosity	Degassing and flashing, no spattering or visible porosity
VFA 658 Medium N, low S	No degassing or visible porosity, smooth profile	No degassing or visible porosity, smooth profile	No degassing or visible porosity, smooth profile	Limited bubble formation, smooth profile, no visible porosity	Pool slightly unstable, degree of degassing, no visible porosity	Pool slightly unstable, degree of degassing, periodic flashing, no visible porosity	Severe spattering and degassing, some visible porosity	Severe spattering and degassing, visible porosity	Severe spattering and degassing, visible porosity	Severe spattering and degassing, visible porosity
VFA 659 High N, low S	Limited periodic instability, smooth weld profile, no visible porosity	Limited bubble formation and spattering, smooth profile, no porosity	Severe spattering and degassing, no visible porosity	Severe spattering and degassing, no visible porosity	Severe spattering and degassing, no visible porosity	Severe spattering and degassing, no visible porosity	Severe spattering and degassing, some visible porosity	Severe spattering and degassing, visible porosity	Severe spattering and degassing, visible porosity	Severe spattering and degassing, visible porosity
VFA 752 Low N, high S	No degassing or visible porosity, smooth profile	No degassing or visible porosity, smooth profile	Limited bubble formation, smooth profile, no visible porosity	Limited bubble formation, smooth profile, no porosity	Limited bubble formation, smooth profile, no porosity	Limited bubble formation, pool stable, smooth profile, no visible porosity	Periodic spattering and degassing, uneven weld profile, no visible porosity	Slight bubble formation and instability, no visible porosity, smooth profile	Slight bubble formation and instability, no visible porosity, smooth profile	Degassing, spattering and flashing, uneven weld profile, little visible porosity
VFA 753 Medium N, high S	No degassing or visible porosity, smooth profile	No degassing or visible porosity, smooth profile	Periodic degassing, no visible porosity	Periodic degassing, no visible porosity	Severe spattering and degassing, some visible porosity	Severe spattering and degassing, some visible porosity	Severe spattering and degassing, visible porosity	Severe spattering and degassing, visible porosity	Severe spattering and degassing, visible porosity	Severe spattering and degassing, visible porosity
VFA 755 High N, high S	Limited bubble formation, smooth weld profile, no instability or porosity	Severe spattering and degassing, no visible porosity	Severe spattering and degassing, no visible porosity	Severe spattering and degassing, some visible porosity	Severe spattering and degassing, some visible porosity	Severe spattering and degassing, some visible porosity	Severe spattering and degassing, visible porosity	Severe spattering and degassing, visible porosity	Severe spattering and degassing, visible porosity	Severe spattering and degassing, visible porosity

Table 4.3 Minimum shielding gas nitrogen content required to initiate steady-state behaviour and bubble formation (percentage by mass).

Alloy	Comments	Minimum shielding gas nitrogen content required to initiate degassing	Corresponding weld metal nitrogen content
VFA 657	Low N, low S	4,5 %	0,160%
VFA 658	Medium N, low S	2,5 %	0,200%
VFA 659	High N, low S	1,5 %	0,250%
VFA 752	Low N, high S	4,0 %	0,172%
VFA 753	Medium N, high S	1,5 %	0,160%
VFA 755	High N, high S	1,0 %	0,290%
AISI 304	-	3,0 %	0,220%

From the results shown in Table 4.3, it is evident that the minimum shielding gas nitrogen content required to initiate steady-state behaviour in the experimental alloys is a function of both the base metal nitrogen content of the alloy and the surface active element concentration. The results show that the weld metal saturation limit is reached at progressively lower shielding gas nitrogen contents as the base metal nitrogen level increases. This again confirms that the base metal nitrogen participates in the nitrogen absorption and desorption reactions during welding. Less nitrogen is required in the shielding gas to reach the saturation limit and initiate steady-state behaviour in the high sulphur alloys because an appreciable fraction of the nitrogen already present in the base metal is prevented from escaping by the higher level of surface coverage. A significant amount of the nitrogen present in the base metal prior to welding is therefore available to participate in the nitrogen absorption/desorption reactions in addition to any nitrogen absorbed from the shielding gas during welding. This is in agreement with the earlier results of this investigation and the conclusions of Arata *et al*[14] described in §4.2.2 above.

In the case of Cromanite, severe nitrogen degassing was evident even in the absence of nitrogen in the shielding gas during welding. This is consistent with the results shown above, which indicate that degassing initiates at lower shielding gas nitrogen levels as the base metal nitrogen content increases. The initial nitrogen content of Cromanite therefore appears to be sufficient to cause nitrogen degassing and to initiate steady-state behaviour in pure argon shielding gas.

4.4 CONCLUSIONS

- Nitrogen absorption and desorption processes in the presence of nitrogen-containing shielding gas during the autogenous welding of stainless steel do not obey Sievert's law. The weld metal nitrogen content initially increases with an increase in the shielding gas nitrogen content at low nitrogen partial pressures. At higher partial pressures a dynamic equilibrium is created where the amount of nitrogen absorbed by the weld metal is balanced by the amount of nitrogen evolved from the weld pool during welding.

- The nitrogen content of autogenous stainless steel welds is a function of the nitrogen partial pressure in the shielding gas, the base metal nitrogen content and the surface active element concentration in the weld metal. In alloys with low surface active element concentrations, the steady-state nitrogen content of the weld metal is not influenced to any significant extent by the base metal nitrogen content. In the case of alloys with high surface active element concentrations, an increase in the base metal nitrogen content results in higher weld metal nitrogen contents over the entire range of nitrogen partial pressures evaluated, including a significant increase in the steady-state nitrogen concentration. It is postulated that the surface active element concentration in the weld metal influences the nitrogen absorption and desorption rates by occupying surface sites required for the absorption of monatomic nitrogen from the arc plasma and the recombination of nitrogen atoms to form N_2 (desorption).
- The minimum shielding gas nitrogen content required to initiate steady-state behaviour and nitrogen bubble formation in the experimental alloys is also a function of the base metal nitrogen content of the alloy and the surface active element concentration. The weld metal saturation limit is reached at progressively lower shielding gas nitrogen contents as the base metal nitrogen level increases. It is postulated that less nitrogen is required in the shielding gas to reach the saturation limit in the high sulphur alloys because an appreciable fraction of the nitrogen already present in the base metal is prevented from escaping by the higher level of surface coverage.

The next chapter describes a kinetic model developed to examine and test the hypotheses developed in this chapter. The model aims at quantifying the influence of the base metal nitrogen content and the surface active element concentration on the rate of the nitrogen absorption and desorption reactions during welding.

4.5 REFERENCES

1. A.A. Howe, "Estimation of liquidus temperatures for steels". Iron and Steelmaking, vol. 15, no. 3. 1988. pp. 134-142.
2. T. Kuwana, H. Kokawa, and K. Naitoh, "The nitrogen absorption of stainless steel weld metal during gas tungsten arc welding". Transactions of the Japan Welding Society, vol. 17, no. 2. October 1986. pp. 117-123.
3. W.S. Bennett, and G.S. Mills, "GTA weldability studies on high manganese stainless steels". Welding Journal, vol. 53, no. 12. 1974. pp. 548s-553s.
4. H. Wada, and R.D. Pehlke, "Solubility of nitrogen in liquid Fe-Cr-Ni alloys containing manganese and molybdenum". Metallurgical Transactions B, vol. 8B. December 1977. pp. 675-682.
5. P.D. Blake, and M.F. Jordan, "Nitrogen absorption during the arc melting of iron". Journal of the Iron and Steel Institute. March 1971. pp. 197-200.
6. V.I. Lakomskii, and G.F. Torkhov, "Absorption of nitrogen from a plasma by liquid metal". Soviet Physics - Doklady, vol. 13, no. 11. May 1969. pp. 1159-1161.
7. T. Kuwana, and H. Kokawa, "The nitrogen absorption of iron weld metal during gas tungsten arc welding". Transactions of the Japan Welding Society, vol. 17, no. 1. April 1986. pp. 20-26.
8. G. den Ouden, and O. Griebling, "Nitrogen absorption during arc welding". Proceedings of the 2nd International Conference on Trends in Welding Research, Gatlinburg, USA. 14-18 May 1989. ASM International. pp. 431-435.

9. A. Bandopadhyay, A. Banerjee, and T. DebRoy, "Nitrogen activity determination in plasmas". Metallurgical Transactions B, vol. 23B. April 1992. pp. 207-214.

10. J.D Katz, and T.B. King, "The kinetics of nitrogen absorption and desorption from a plasma arc by molten iron". Metallurgical Transactions B, vol. 20B. April 1989. pp. 175-185.

11. R.K. Okagawa, R.D. Dixon, and D.L. Olson, "The influence of nitrogen from welding on stainless steel weld metal microstructures". Welding Journal, vol. 62, no. 8. August 1983. pp. 204s-209s.

12. N. Suutala, "Effect of manganese and nitrogen on the solidification mode in austenitic stainless steel welds". Metallurgical Transactions A, vol. 13A. December 1982. pp. 2121-2130.

13. T.D. Battle, and R.D. Pehlke, "Kinetics of nitrogen absorption and desorption by liquid iron and iron alloys". Ironmaking & Steelmaking, vol. 13, no. 4. 1986. pp. 176-189.

14. Y. Arata, F. Matsuda, and S. Saruwatari, "Varestraint test for solidification crack susceptibility in weld metal of austenitic stainless steels". Transactions of the JWRI, vol. 3. 1974. pp. 79-88.